J. Am. Chem. Soc. **1991**, *113*, 8257–8262

Anisotropic Indirect Spin–Spin Coupling in the Solid State. Experimental Evidence of Noncontact Contributions to ${}^1J({}^{31}P,{}^{199}Hg)$

William P. Power, Michael D. Lumsden, and Roderick E. Wasylishen*

Contribution from the Department of Chemistry, Dalhousie University, Halifax, Nova Scotia B3H 4J3, Canada. *Received May 6, 1991*

Abstract: Anisotropies in the ${}^{31}P$ chemical shift tensor and the ${}^{31}P$–${}^{199}Hg$ indirect spin–spin coupling tensor for a series of mercury phosphines, $[HgPR_3(NO_3)_2]_2$, have been determined from their ${}^{31}P$ solid-state NMR line shapes. The principal components of the ${}^{31}P$ chemical shift tensor vary over a total range of 125 ppm for the different mercury phosphines, but the component that is along or nearest to the P–Hg bond is relatively invariant. The indirect spin–spin coupling tensor involving ${}^{31}P$ and ${}^{199}Hg$, ${}^1J({}^{31}P,{}^{199}Hg)$, exhibits considerable anisotropy, of greater than 5 kHz in most cases. These results indicate that mechanisms other than the contact term are in part responsible for the transfer of nuclear-spin information between ${}^{31}P$ and ${}^{199}Hg$ in these compounds.

Introduction

Indirect spin–spin (J) couplings between ${}^{31}P$ and various metal nuclei (M) such as ${}^{109}Ag$, ${}^{195}Pt$, and ${}^{199}Hg$ have been used to derive structural information of coordination compounds from solution NMR spectra over the last 20 years.[1–4] For a given class of compounds, the values of ${}^1J(M,{}^{31}P)$ often have been found to correlate with a variety of properties, such as metal–phosphorus bond lengths, bond angles at the metal center, and electronegativity of trans ligands, among others. Interpretations of these couplings have been based exclusively on the contact mechanism for electron-mediated communication between the two nuclear spins involved, which, following McConnell,[5] can be described by eq 1, where ${}^3\Delta E$ is the average triplet excitation energy, $s_M(0)$ and

$$ {}^1J(M,{}^{31}P) = \left(\frac{\mu_0}{3\pi}\right)^2 \mu_B{}^2 h\gamma_M\gamma_P({}^3\Delta E)^{-1}|s_M(0)|^2|s_P(0)|^2P^2_{s_Ms_P} \qquad (1) $$

$s_P(0)$ are the magnitudes of the s orbitals precisely at the metal and phosphorus nuclei, respectively, $P_{s_Ms_P}$ is the molecular orbital (MO) bond order between the two nuclei, and all other terms are standard constants. This simple equation involves a number of approximations, as previously described by Pidcock,[3] not least of which is the assumption that the J coupling depends exclusively on the Fermi contact mechanism. The apparent success of this equation in rationalizing various experimental trends in metal–phosphorus couplings has led to the belief that experimental values of J_{iso} provide a measure of the degree of s-orbital character in the bond between two nuclei. However, the original theoretical description of J coupling provided by Ramsey[6] was more complex and involved not only the Fermi contact mechanism but several others as well. In his formulation, the overall indirect spin–spin coupling tensor was made up of four terms

$$ \boldsymbol{J} = \boldsymbol{J}_{OB} + \boldsymbol{J}_{SD} + \boldsymbol{J}_{FC} + \boldsymbol{J}_{FC\times SD} \qquad (2) $$

where OB, SD, and FC correspond to orbital, spin-dipolar, and Fermi contact contributions, respectively. The final contribution arises from a cross-term in second-order perturbation theory between the Fermi contact and spin-dipolar mechanisms.

The orbital contribution to $\boldsymbol{J}$ results from the interaction between the magnetic moments of the nuclei and the orbital angular momentum of the surrounding electrons. The spin-dipolar mechanism involves a coupling between the nuclear spins and electron spins at a finite distance from the nucleus. The Fermi contact is similar to the spin-dipolar term, except that it depends on electron density precisely at the nuclei involved. The similar origin of these latter two terms gives rise to the cross-term between them. Of the four contributions to the indirect spin–spin coupling, all except the contact–spin-dipolar cross-term contribute to the isotropic value of $\boldsymbol{J}$ (i.e., this latter term is traceless); conversely, only the Fermi contact term does not contribute to the anisotropy in $\boldsymbol{J}$, as its dependence on s-electron density at the nucleus precludes any orientation dependence. Thus, according to the theory of Ramsey, the anisotropy of $\boldsymbol{J}$ should be precisely zero if the exclusive mechanism for spin–spin coupling is the Fermi contact mechanism.[7]

Over the past 15 years, a relativistic analogue to Ramsey's theory of spin–spin coupling has been developed by Pyykkö.[8] Relativistic effects have been found to be important in the theoretical treatment of the heavier elements, due to the high velocities of the electrons near the massive and highly charged nuclei.[9] The relativistic expression for indirect spin–spin coupling involves only one Hamiltonian; however, it is possible to extract terms that, at their nonrelativistic limits, roughly correspond to Ramsey's expressions. Although the spin-dipolar and orbital analogues cannot be explicitly separated, residing together in Pyykkö's $\boldsymbol{J}_{p-p}$ and $\boldsymbol{J}_{\sigma-\pi}$ terms, a contact contribution, J_{s-s}, does appear, which again depends on s-electron density at the nuclei involved, and is completely isotropic. Another relativistic term, $\boldsymbol{J}_{s-p}$, is traceless, but does contribute to the anisotropy in $\boldsymbol{J}$. Clearly, in relativistic theory, as in Ramsey's theory, the presence of any anisotropy in $\boldsymbol{J}$ indicates that the contact term is not the sole mechanism for indirect spin–spin coupling.

Reliable experimental determinations of the $\boldsymbol{J}$ tensor, and more specifically anisotropies of $\boldsymbol{J}$, are scarce in the literature.[10–14] In general, this can be attributed to difficulties in measuring ΔJ. In

---

* Author to whom correspondence should be addressed.

(1) Nixon, J. F.; Pidcock, A. *Annu. Rev. NMR Spectrosc.* **1969**, *2*, 345.

(2) Pregosin, P. S.; Kunz, R. W. *${}^{31}P$ and ${}^{13}C$ NMR of Transition Metal Phosphine Complexes*; *NMR Basic Principles and Progress*; Vol. 12; Springer-Verlag: Berlin, 1979.

(3) Pidcock, A. In *Catalytic Aspects of Metal Phosphine Complexes*; Alyea, E. C., Meek, D. W., Eds.; Advances in Chemistry Series 196; American Chemical Society: Washington, DC, 1982; pp 1–22.

(4) Verkade, J. G.; Mosbo, J. A. In *Phosphorus-31 NMR Spectroscopy in Stereochemical Analysis, Organic Compounds and Metal Complexes*; Verkade, J. G., Quin, L. D., Eds.; Methods in Stereochemical Analysis 8; VCH Publishers, Inc.: Deerfield Beach, FL, 1987; pp 425–463.

(5) McConnell, H. M. *J. Chem. Phys.* **1956**, *24*, 460.

(6) Ramsey, N. F. *Phys. Rev.* **1953**, *91*, 303.

(7) Buckingham, A. D.; Love, I. *J. Magn. Reson.* **1970**, *2*, 338.

(8) Pyykkö, P. *Chem. Phys.* **1977**, *22*, 289.

(9) Pyykkö, P. *Chem. Rev.* **1988**, *88*, 563.

(10) Lounila, J.; Jokisaari, J. *Prog. Nucl. Magn. Reson. Spectrosc.* **1982**, *15*, 249.

(11) Robert, J. B.; Wiesenfeld, L. *Phys. Rep.* **1982**, *86*, 363.

(12) Robert, J. B.; Wiesenfeld, L. In *Phosphorus-31 NMR Spectroscopy in Stereochemical Analysis, Organic Compounds and Metal Complexes*; Verkade, J. G., Quin, L. D., Eds.; Methods in Stereochemical Analysis 8; VCH Publishers, Inc.: Deerfield Beach, FL, 1987; pp 151–183.

(13) Jameson, C. J. In *Phosphorus-31 NMR Spectroscopy in Stereochemical Analysis. Organic Compounds and Metal Complexes*; Verkade, J. G., Quin, L. D., Eds.; Methods in Stereochemical Analysis 8; VCH Publishers, Inc.: Deerfield Beach, FL, 1987; pp 205–230.

(14) Jameson, C. J. In *Multinuclear NMR*; Mason, J., Ed.; Plenum Press: New York, 1987; pp 89–131.

0002-7863/91/1513-8257$02.50/0

isotropic phases, there are no manifestations of anisotropy in J on observed NMR spectra because of rapid molecular tumbling. In ordered or anisotropic phases, such as liquid crystal systems or crystalline solids, ΔJ appears only in combination with the direct dipolar coupling, R_{DD}, resulting in an effective dipolar coupling constant, R_{eff} (eq 3–5).[15] The dipolar coupling constant, R_{DD}

$$\langle R_{eff} \rangle = \langle R_{DD} \rangle - \tfrac{1}{3}\langle \Delta J \rangle \tag{3}$$

$$\langle R_{DD} \rangle = \frac{\gamma_A \gamma_B \hbar}{2\pi \langle r_{AB}{}^3 \rangle} \frac{\mu_0}{4\pi} \tag{4}$$

$$\langle \Delta J \rangle = \langle J_{\parallel} \rangle - \langle J_{\perp} \rangle \tag{5}$$

is dependent only on the inverse cube of the separation of the two nuclei, A and B, which can be determined by other experiments, such as X-ray crystallography. Assuming axial symmetry in the J tensor, the components, $J_{\parallel}$ and $J_{\perp}$, correspond to the magnitudes of J when the A–B bond or internuclear vector is oriented parallel to and perpendicular to the static magnetic field. The angular brackets indicate that each term is averaged over any motion that may be occurring, although these terms may be affected differently.[16]

One popular method used to determine ΔJ values has been to study the NMR spectra of solute molecules oriented in liquid crystal solvents.[10,17] In general, the analysis is complicated because the orientational order tensor, S^D, must be determined. Although only a single-order parameter (one element of S^D) is necessary to describe the orientational order in highly symmetric molecules, the degree of order is low and apparent coupling constants must be corrected for vibrational motions of the solute. In addition, one must account for the orientation-dependent deformations of the solute molecule, induced by the anisotropic forces present in the liquid crystalline matrix.[18,19]

Reliable experimental data concerning anisotropy in J should be available from solid-state NMR. The greatest advantage of this technique is the precise knowledge of the compound's molecular structure, which is afforded by crystallographic data. There should be no doubt as to the suitable comparison of crystallographic and NMR spectroscopic data when the NMR sample is in the same state, as opposed to cases where the results of crystallographic data are assumed to be models of the solute structure in liquid crystalline solvents. The effects of motional averaging also should be eliminated or substantially attenuated in the solid state, especially for large molecules, compared to when they are dissolved in liquid crystal solvents.

With these considerations, we have undertaken a study of the nature of the indirect spin–spin coupling between ^{31}P and ^{199}Hg in a series of mercury phosphines,[20] of the general form $[HgPR_3(NO_3)_2]_2$, where R is an alkyl or aryl group. Compounds of this latter type have been well characterized by both ^{31}P solution NMR[21] and X-ray crystallography.[22-24] In the solid state, these compounds generally form centrosymmetric dimers or polymeric chains containing bridging nitrate groups. In solution NMR studies, they have been found to possess very large isotropic J-(^{31}P,^{199}Hg) coupling constants, of the order of 10 kHz. The direct dipolar coupling constant between these two nuclei is quite small due to their relatively large separation in the P–Hg bond. The combination of a large J_{iso} and a small R_{DD} enhances the possibility of observing any anisotropy in the indirect coupling and of measuring its magnitude without a large margin of error.

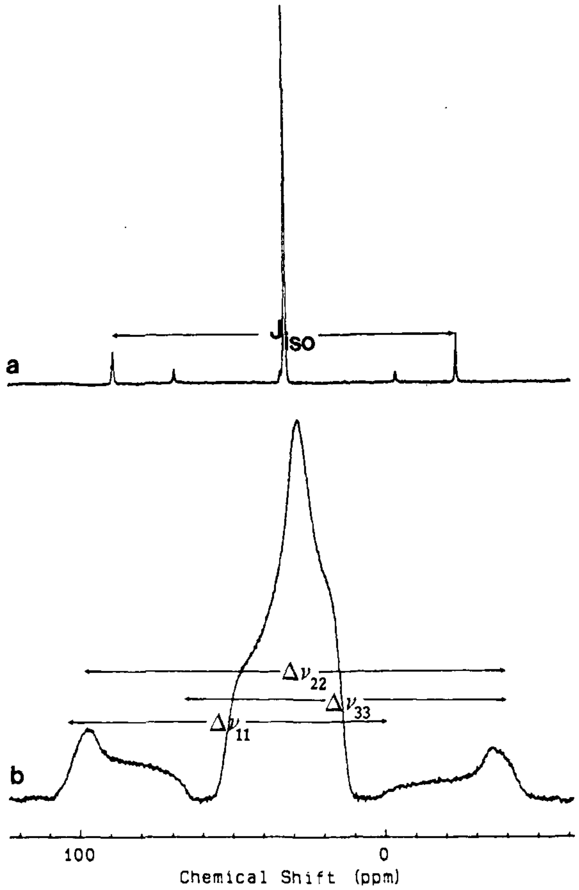

Figure 1. Phosphorus-31 solid-state NMR spectra of $[HgP(m\text{-tolyl})_3(NO_3)_2]_2$: (a) with MAS at 3.0 kHz and (b) static, with the splittings about each of the principal components of the ^{31}P chemical shift tensor indicated.

Experimental Section

The 1:1 mercury(II) nitrate–phosphine complexes were prepared according to literature methods.[21] Products were recrystallized from dichloromethane by slow addition of diethyl ether. All compounds were characterized by melting points and their solution ^{31}P NMR spectra. Solution-state ^{31}P NMR spectra were obtained on a Nicolet NT360 NMR spectrometer at 146.1 MHz.

All solid-state ^{31}P NMR spectra were obtained at 81.0 MHz on a Bruker MSL-200 NMR spectrometer under conditions of cross-polarization (CP) and high-power proton decoupling. Typical pulse widths were 4 μs, with contact times for the cross-polarization sequence lasting 3 ms. Magic-angle spinning (MAS) spectra were obtained at spinning rates up to 4 kHz, using 7-mm-o.d. zirconia rotors in a Bruker double-air-bearing MAS probe. Acquisition times for both static and spinning spectra were 65.54 ms, during which 8192 data points were collected. All spectra were obtained at 293 K and were referenced with respect to 85% H_3PO_4(aq) at 0 ppm, using the ^{31}P signal of external $NH_4H_2PO_4$(s), which occurs at +0.81 ppm.

All simulated spectra were generated using a FORTRAN-77 program developed in this laboratory incorporating the POWDER simulation routine,[25] and all calculations were performed on an 80286/287 microcomputer.

Results

The ^{31}P NMR spectra of all of the mercury phosphines consist of three main spectral features: an intense central feature arising

---

[15] VanderHart, D. L.; Gutowsky, H. S. *J. Chem. Phys.* **1968**, *49*, 261.

[16] Henry, E. R.; Szabo, A. *J. Chem. Phys.* **1985**, *82*, 4753.

[17] Emsley, J. W.; Lindon, J. C. *NMR Spectroscopy Using Liquid Crystal Solvents*; Pergamon Press: Oxford, 1975.

[18] (a) Jokisaari, J.; Hiltunen, Y.; Lounila, J. *J. Chem. Phys.* **1986**, *85*, 3198. (b) Pulkkinen, A.; Hiltunen, Y.; Jokisaari, J. *Liq. Cryst.* **1988**, *3*, 737. (c) Lounila, J.; Ala-Korpela, M.; Jokisaari, J. *J. Chem. Phys.* **1990**, *93*, 8514.

[19] (a) Lounila, J.; Diehl, P. *J. Magn. Reson.* **1984**, *56*, 254. (b) Lounila, J.; Diehl, P. *Mol. Phys.* **1984**, *52*, 827. (c) Lounila, J.; *Mol. Phys.* **1986**, *58*, 897.

[20] Penner, G. H.; Power, W. P.; Wasylishen, R. E. *Can. J. Chem.* **1988**, *66*, 1821.

[21] Alyea, E. C.; Dias, S. A.; Goel, R. G.; Ogini, W. O.; Pilon, P.; Meek, D. W. *Inorg. Chem.* **1978**, *17*, 1697.

[22] Whitlow, S. H. *Can. J. Chem.* **1974**, *52*, 198.

[23] Alyea, E. C.; Dias, S. A.; Ferguson, G.; Restivo, A. J. *Inorg. Chem.* **1977**, *16*, 2329.

[24] Alyea, E. C.; Dias, S. A.; Ferguson, G.; Parvez, M. *Inorg. Chim. Acta* **1979**, *37*, 45.

[25] Alderman, D. W.; Solum, M. S.; Grant, D. M. *J. Chem. Phys.* **1986**, *84*, 3717.

from ^{31}P nuclei that are bonded to Hg isotopes which do not possess nuclear spin $I = {}^1/_2$ and two satellites, each with approximately 10% of the intensity of the central feature, arising from ^{31}P nuclei which are adjacent to ^{199}Hg nuclei (16.84% natural abundance, $I = {}^1/_2$). The satellites are displaced to either side of the central feature due to the large indirect spin–spin coupling (J coupling) between ^{31}P and ^{199}Hg. Spectra obtained under conditions of rapid magic-angle spinning (MAS), as portrayed in Figure 1a for $[\mathrm{HgP}(m\text{-tolyl})_3(\mathrm{NO}_3)_2]_2$, resemble what is observed in solution, with sharp peaks at frequencies corresponding to the ^{31}P isotropic chemical shift, δ_{iso}, and at $\delta_{\mathrm{iso}} \pm {}^1/_2 J_{\mathrm{iso}}$ for those ^{31}P nuclei adjacent to ^{199}Hg nuclei ($m_{\mathrm{Hg}} = \pm{}^1/_2$). Thus, isotropic values for the ^{31}P chemical shift and the ^{31}P–^{199}Hg J coupling in the solid state are readily determined.

When spectra of the static powder samples are obtained, orientation-dependent signals, such as those shown in Figure 1b, are observed, which depend on the anisotropic nature of the chemical shift for the central feature and on the combined anisotropic effects of the chemical shift and direct dipolar coupling as well as any anisotropy in $\boldsymbol{J}$ that may be present for the satellites.[15] The ^{31}P NMR line shape can be described by

$$\nu_{\mathrm{central}}(\theta,\phi) = \nu_0 - \nu_{\mathrm{CS}}(\theta,\phi) \tag{6}$$

$$\nu_{\mathrm{satellite}}(\theta,\phi) = \nu_0 - \nu_{\mathrm{CS}}(\theta,\phi) - m_{\mathrm{Hg}}[\nu_{\mathrm{DJ}}(\theta,\phi) - {}^1J_{\mathrm{iso}}({}^{31}\mathrm{P},{}^{199}\mathrm{Hg})] \tag{7}$$

where

$$\nu_0 = \frac{\gamma_{\mathrm{P}} \boldsymbol{B}_0}{2\pi}$$

$$\nu_{\mathrm{CS}}(\theta,\phi) = \nu_0(\sigma_{11} \sin^2\theta \cos^2\phi + \sigma_{22} \sin^2\theta \sin^2\phi + \sigma_{33} \cos^2\theta)$$

and

$$\nu_{\mathrm{DJ}}(\theta,\phi) = \left(\frac{\gamma_{\mathrm{P}}\gamma_{\mathrm{Hg}}\hbar}{2\pi\langle r_{\mathrm{P-Hg}}{}^3\rangle}\,\frac{\mu_0}{4\pi} - {}^1\!/_3\Delta J({}^{31}\mathrm{P},{}^{199}\mathrm{Hg})\right)(3\cos^2\theta - 1)$$

The principal components of the ^{31}P chemical shielding tensor, σ_{ii}, $i = 1$–3, are reported most commonly as chemical shifts, δ_{ii}, with respect to a reference. We maintain the convention that δ_{11} and δ_{33} denote the shifts of the least shielded and most shielded principal components, respectively. Equation 7 assumes that $\boldsymbol{J}$ is axially symmetric and that $J_{\parallel}$ lies along the P–Hg bond. As described elsewhere, the above equations must be generalized to account for the relative orientations of the ^{31}P chemical shielding and ^{31}P,^{199}Hg spin–spin coupling interactions in the molecular frame.[15,26,27] The angles θ and ϕ orient the magnetic field vector, $\mathbf{B}_0$, in the principal axis system of the chemical shielding tensor, where θ is the angle between σ_{33} and $\mathbf{B}_0$, and ϕ is the angle between σ_{11} and the projection of $\mathbf{B}_0$ onto the σ_{11}–σ_{22} plane. The P–Hg internuclear vector, $\mathbf{r}_{\mathrm{P-Hg}}$, is oriented in this reference frame using the Euler angles α and β, such that the angular term, $(3\cos^2\theta - 1)$, in the expression for ν_{DJ} is replaced by

$$(3(\sin\theta \sin\beta \cos(\alpha - \phi) + \cos\theta \cos\beta)^2 - 1)$$

The angle between σ_{33} and $\mathbf{r}_{\mathrm{P-Hg}}$ is given by β, while α denotes the angle between σ_{11} and the projection of $\mathbf{r}_{\mathrm{P-Hg}}$ onto the σ_{11}–σ_{22} plane. After this modification, eqs 6 and 7 can be used to simulate the experimental static spectra, providing the magnitudes and relative orientations of the relevant interactions. The results of such analyses for the 1:1 mercury nitrate–phosphine complexes are presented in Table I.

Table I. Phosphorus-31 NMR Parameters[a] for Solid $[\mathrm{HgPR}_3(\mathrm{NO}_3)_2]_2$

R	δ_{iso}	δ_{11}	δ_{22}	δ_{33}	$^1J_{\mathrm{iso}}(^{31}\mathrm{P}, {}^{199}\mathrm{Hg})$	ΔJ
phenyl	32.2	44.2	34.6	$\underline{17.7}$	9572	4545
o-tolyl[b]	3.6	$\underline{29.1}$	−9.2	−9.2	9660	5205
m-tolyl	32.6	54.1	$\underline{28.4}$	15.7	9165	5235
p-tolyl	40.3	72.8	27.1	$\underline{20.7}$	9144	5470
mesityl[c]	3.2	$\underline{10.2}$	4.4	−5.0	10468	5560
	1.9	$\underline{9.2}$	2.1	−5.6	10566	5560
p-MeOPh[c]	42.2	68.3	40.8	$\underline{17.4}$	9327	4765
	36.7	52.1	36.8	$\underline{21.1}$	9309	3740
cyclohexyl	79.5	114.9	91.3	$\underline{32.5}$	8008	5525

[a] Chemical shifts are given (ppm) from 85% $\mathrm{H_3PO_4}$(aq), and J coupling parameters are expressed in hertz. The underline indicates the component of the ^{31}P chemical shift tensor that lies along or closest to the P–Hg bond. In all cases, the values for ΔJ were determined assuming that the dipolar coupling constant between ^{31}P and ^{199}Hg was 645 Hz, which corresponds to a P–Hg bond length of 2.385 Å. Errors in δ_{iso} and J_{iso} are ±0.2 ppm and ±15 Hz, respectively; the errors in δ_{ii} ($i = 1$–3) are less than 2.0 ppm. Errors in ΔJ are ±200 Hz, except as otherwise noted in the text. [b] From ref 20. [c] Determined from analysis of the slow-spinning MAS spectrum.

The large values of $^1J_{\mathrm{iso}}(^{31}\mathrm{P},{}^{199}\mathrm{Hg})$ in the mercury phosphines permit unobscured observation of the central and satellite regions of the spectra, greatly facilitating their analysis. The three principal components of the ^{31}P chemical shielding tensor can be directly determined from the central feature and used to interpret the satellite line shapes. The values determined for the three principal components of the ^{31}P chemical shift tensor for each of the compounds are given in Table I. The only remaining unknown parameters required to characterize the satellites are the orientation of the ^{31}P chemical shielding tensor and the effective dipolar coupling constant, which includes the effects of any anisotropy in $\boldsymbol{J}$. The orientation of the shielding tensor in the molecular frame is readily identified from these powder patterns. The splittings of the three singularities of the satellites about those of the central feature are due to the combined influence of J_{iso} and R_{eff}; that of maximum splitting, $|2R_{\mathrm{eff}} - J_{\mathrm{iso}}|$, will correspond to an orientation where that component of the shielding tensor is along the P–Hg bond, while the other two splittings, which should correspond to $|R_{\mathrm{eff}} + J_{\mathrm{iso}}|$, denote orientations of the shielding tensor perpendicular to the P–Hg bond.[15] If none of the principal components of the ^{31}P chemical shielding tensor lie directly along the P–Hg bond, the values of these splittings will be slightly modified. However, in all compounds discussed here, it was found that one component of the shielding tensor was along, or very close to, the P–Hg bond. For example, in $[\mathrm{HgP}(m\text{-tolyl})_3(\mathrm{NO}_3)_2]_2$ (Figure 1b), it is clear that the direction of maximum splitting about each of the three principal components of the central line shape is $\Delta\nu_{22}$, corresponding to splitting about the intermediate shielding component, δ_{22}, while the splittings about the other two components are approximately equal. The chemical shift values underlined in Table I indicate the principal component of the ^{31}P chemical shift tensor, which was determined to lie along or close to the P–Hg bond in each compound.

Once values of R_{eff} are determined from the satellite line shapes, estimates of the anisotropy in J (ΔJ) are obtained from two further pieces of information: the absolute sign of $^1J_{\mathrm{iso}}(^{31}\mathrm{P},{}^{199}\mathrm{Hg})$ and values of the P–Hg bond length as determined by X-ray crystallography. The sign of the one-bond coupling between ^{31}P and ^{199}Hg in various mercury–phosphorus compounds has always been determined to be positive.[4,14,28,29] The absolute sign of J_{iso} limits the possible values of ΔJ that would be consistent with the observed line shape. The P–Hg bond length of 2.385 Å was used to derive the direct dipolar coupling constant, $R_{\mathrm{DD}} = 645$ Hz, in the absence of influences due to motional averaging. This value for $r_{\mathrm{P-Hg}}$ corresponds to an average bond length determined from three crystal structures for compounds of the general form $[\mathrm{HgPR}_3(\mathrm{NO}_3)_2]_2$: R = PPh_3, $r_{\mathrm{P-Hg}} = 2.359$ Å;[22] R = PCy_3 (2.359 Å);[23]

---

(26) Zilm, K. W.; Grant, D. M. *J. Am. Chem. Soc.* **1981**, *103*, 2913.

(27) Power, W. P.; Wasylishen, R. E. *Annu. Rep. NMR Spectrosc.* **1991**, *23*, 1.

(28) McFarlane, W.; Rycroft, D. S. *J. Chem. Soc., Faraday Trans. 2*, **1974**, *70*, 377.

(29) Goggin, P. L.; Goodfellow, R. J.; McEwan, D. M.; Griffiths, A. J.; Kessler, K. *J. Chem. Res., Miniprint* **1979**, 2315.

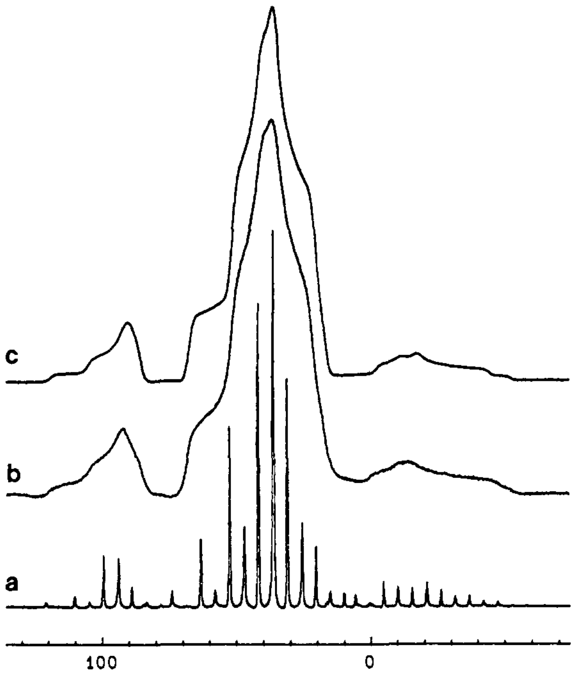

Figure 2. Phosphorus-31 solid-state NMR spectra of [HgP(p-methoxyphenyl)$_3$(NO$_3$)$_2$]$_2$: (a) with slow MAS (ν_r = 862 Hz), (b) static, and (c) calculated static, from parameters derived from fitting of the MAS sidebands.

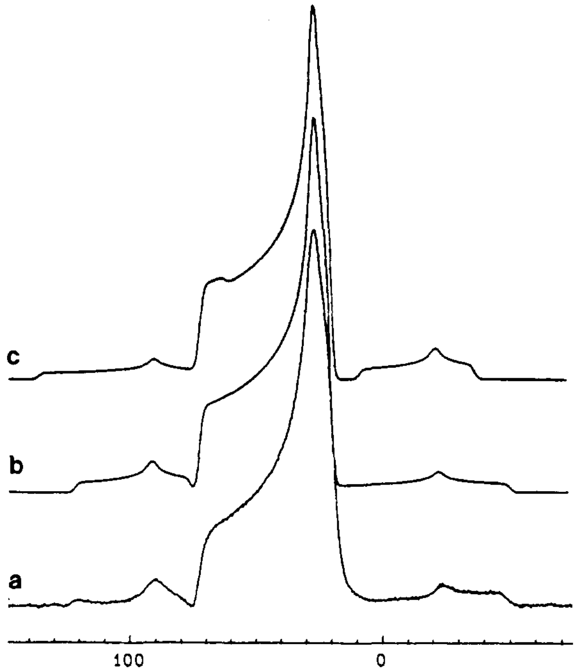

Figure 3. Phosphorus-31 solid-state NMR line shapes of [HgP(p-tolyl)$_3$(NO$_3$)$_2$]$_2$: (a) experimental and calculated spectra with J_{iso}, ΔJ values of (b) +9144 Hz, +5470 Hz or −9144 Hz, −1600 Hz, and (c) +9144 Hz, −1600 Hz or −9144 Hz, +5470 Hz.

R = PMes$_3$, 2.395 and 2.418 Å.[24] Crystallographic data that exist for other similar compounds, with acetate[30] or thiocyanate[31] anions, indicate P–Hg bond lengths falling within the range for the above nitrate derivatives. Thus, the variation in $r_{\text{P-Hg}}$ in these mercury phosphines is probably less than ±0.04 Å, which corresponds to a deviation in R_{DD} of ±33 Hz. A reduction in R_{DD} of an equal amount due to libration of the P–Hg bond would require motion through a cone with a half-angle of 10.4° about the equilibrium position,[16,26] which would be quite substantial motion for these heavy nuclei within a large molecule. The X-ray data discussed previously do not provide evidence for motion of this order in this class of compounds. Thus, it can be seen that the estimate for R_{DD} given here is quite robust with respect to the possible sources of error in its derivation.

The values of ΔJ given in Table I are the results determined within the bounds outlined above. It should be noted that any error in the estimate of R_{DD} will be multiplied by 3 in the derivation of ΔJ (see eq 3); however, that source of error has been limited to (±33 Hz) × 3 = ±99 Hz. Overall uncertainties in the values of ΔJ given in Table I are ±200 Hz, except for [HgP(phenyl)$_3$(NO$_3$)$_2$]$_2$, due the presence of some impurities, including the 2:1 phosphine–mercury(II) nitrate complex. Also, larger errors in ΔJ are given for [HgP(p-methoxyphenyl)$_3$(NO$_3$)$_2$]$_2$ and [HgP(mesityl)$_3$(NO$_3$)$_2$]$_2$, due to the presence of two nonequivalent ^{31}P sites in powder samples of each. Errors in ΔJ for the p-methoxyphenyl compound are ±250 and ±375 Hz for the two sites, respectively, and are ±500 Hz for the triphenylphosphine compound and for each site in the trimesitylphosphine compound. The two-component spectra of the p-methoxyphenyl and mesityl compounds were analyzed with use of a Herzfeld–Berger fitting[32] of the ^{31}P slow MAS NMR spectra (e.g., Figure 2a). The values for ΔJ for the two sites in the mesityl compound were identical within experimental error. Slow-spinning MAS experiments allow the spinning sidebands of each site to be resolved and then separately analyzed, which is not possible with the static spectra due to considerable overlap of the spectral features. The resulting parameters determined from the MAS spectra were used to generate a calculated spectrum of each static powder sample, which gave excellent fits to the experimental line shapes, an example of which is given in Figure 2. The X-ray crystal structure for the trimesitylphosphine compound[24] demonstrates the presence of two distinct centrosymmetric dimers in the unit cell, which is in agreement with the observation of two peaks of equal intensity in the ^{31}P MAS NMR spectrum. It is unclear whether the presence of two signals in the ^{31}P solid-state NMR spectra of the [tris(p-methoxyphenyl)phosphine]mercury(II) complex are due to two crystallographically distinct sites within the unit cell or two different types of crystals in the bulk powder sample. That the two signals are equally intense indicates that the former case is more likely, although crystallographic data would prove useful in distinguishing the proper choice for this compound.

Although there are two possible choices for ΔJ depending on the sign that one chooses for R_{eff}, only one of the choices is reasonable. Presented in Figure 3 are two calculated ^{31}P NMR powder spectra for the tri-p-tolylphosphine derivative as well as the experimental line shape. Quite clearly, one calculated spectrum, corresponding to J_{iso}, ΔJ values of +9144 Hz, +5470 Hz or −9144 Hz, −1600 Hz, fits the experimental better than the other, +9144 Hz, −1600 Hz or −9144 Hz, +5470 Hz. However, as this fixes only the relative signs of J_{iso} and ΔJ, further information is required to identify the proper choice for ΔJ. The previous experimental determination of the sign of $^1J_{iso}(^{31}\text{P},^{199}\text{Hg})$ as positive[28,29] then allows the proper discrimination between the two possibilities to be made. It is in this fashion that the values for ΔJ in Table I have been determined.

It should be noted that analysis of the values for R_{eff} obtained from the spectra for these mercury(II) phosphines assuming ΔJ = 0 yields values for $r_{\text{P-Hg}}$ of approximately 1.95 Å and indicates that $^1J_{iso}(^{31}\text{P},^{199}\text{Hg})$ is negative. Both of these conclusions are in complete disagreement with previous findings, demonstrating that anisotropy in J must be present. In order to demonstrate how ΔJ influences the ^{31}P NMR powder line shapes, we have illustrated in Figure 4 the calculated spectra that are obtained for different values of ΔJ, using the parameters corresponding to the observations for the (tri-o-tolylphosphine)mercury compound

---

(30) (a) Roberts, P. J.; Ferguson, G.; Goel, R. G.; Ogini, W. O.; Restivo, R. J. *J. Chem. Soc., Dalton Trans.* **1978**, 253. (b) Alyea, E. C.; Dias, S. A.; Ferguson, G.; Khan, M. A.; Roberts, P. J. *Inorg. Chem.* **1979**, *18*, 2433.

(31) Alyea, E. C.; Ferguson, G.; Restivo, R. J. *J. Chem. Soc., Dalton Trans.* **1977**, 1845.

(32) Herzfeld, J.; Berger, A. E. *J. Chem. Phys.* **1980**, *73*, 6021.

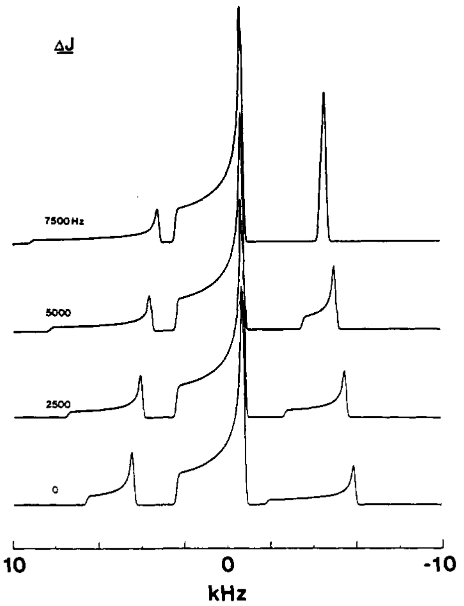

Figure 4. Calculated ^{31}P NMR line shapes of $[HgP(o\text{-tolyl})_3(NO_3)_2]_2$ for values for ΔJ of 0, 2500, 5000, and 7500 Hz, as indicated.

for the other variables in the calculation. This clearly shows the influence of the anisotropy in the indirect spin–spin coupling between ^{31}P and ^{199}Hg on the ^{31}P NMR powder line shape for these compounds.

Discussion

The isotropic values of the ^{31}P chemical shift and the ^{31}P–^{199}Hg indirect spin–spin coupling in the solid state for the mercury(II) phosphines are near the values obtained previously for these compounds in solution.[21] This indicates that there are probably no significant changes in the structure of these compounds on going from solution to the solid state. However, the solid-state NMR spectral data provide a more reliable basis upon which to make comparisons to crystallographic results, as well as giving a more detailed portrayal of the origin of the structural influences on chemical shielding and J coupling, by exhibiting the anisotropic nature of these interactions. It also eliminates the effects due to exchange of ligands in solution, although steric influences may be amplified in the solid state due to crystal-packing forces.

It is apparent from Table I that the ^{31}P chemical shielding parameters in these compounds are widely varied, as the principal components span a spectral range of approximately 125 ppm. However, the principal component of the ^{31}P chemical shift tensor, which was determined to lie along the P–Hg bond, was relatively constant, only varying from 9.2 to 32.5 ppm. This indicates that, in these compounds, the electronic environments about the ^{31}P nuclei in the plane perpendicular to the P–Hg bond are similar, at least much more so than in the other directions. The variability in the ^{31}P chemical shift for different phosphine ligands in the mercury phosphines is similar to that observed in the free phosphines themselves.[33] However, the orientations of the ^{31}P chemical shift tensor in several free phosphines were based on symmetry arguments and could not be determined with certainty. The magnitude of the ^{31}P coordination shift in the solid state, which is the difference in isotropic chemical shifts of the free phosphine and the phosphine bonded to mercury, ranged from 35 to 72 ppm. The phosphines with aryl ligands had similar coordination shifts, with a range of only 35–57 ppm. A somewhat larger coordination shift of 72 ppm was observed for the tricyclohexylphosphine derivative. In all cases, the coordination shift was in the high-frequency (down-field) direction.

The values for ΔJ are relatively constant, 5400 ± 200 Hz, with the exception of the results for $[HgPPh_3(NO_3)_2]_2$ and $[HgP(p\text{-methoxyphenyl})_3(NO_3)_2]_2$, while the isotropic indirect spin–spin coupling constants vary from 10566 to 8008 Hz. This result establishes the presence of substantial anisotropy in J involving ^{31}P and ^{199}Hg, in contrast with previous assumptions and calculations that proposed that the Fermi contact mechanism is responsible for at least 98% of the observed indirect spin–spin interaction.[34] It should be noted that Allman and Lenkinski were unsuccessful in establishing a correlation between parameters related to the Fermi contact interpretations and $^1J_{iso}(^{31}P,^{199}Hg)$ in the $Hg(PR_3)_2X_2$ series of compounds in the solid state.[35] We have also provided evidence of noncontact contributions to the indirect spin–spin coupling between ^{31}P and ^{199}Hg in solid mercury phosphonates.[36] The anisotropies in J were significantly smaller than the values determined here, even though the values of J_{iso} were larger. This could be due to the "harder" nature of the phosphonate ligand compared to the phosphine. One aspect of the data in Table I that remains unclear is the apparent uniformity of values for ΔJ in these compounds. Perhaps this reflects a dominance of the contact mechanism in *variations* of the observed $J_{iso}(^{31}P,^{199}Hg)$. However, there are as yet insufficient data to draw definite conclusions; the values for the phenyl and *p*-methoxyphenyl compound do not appear to follow this trend. Clearly, theoretical calculations of $^1J_{iso}(^{31}P,^{199}Hg)$ in these mercury–phosphorus compounds would be useful in indicating the extent of contact contributions to and the sources of the anisotropy in the indirect spin–spin coupling. However, the complexity of these heavy-atom systems may preclude reliable theoretical calculations of J couplings for some time.

Anisotropies in the indirect coupling between ^{31}P and other nuclei have been previously reported in the literature. In ^{31}P single-crystal studies of two tetraalkyldiphosphine disulfides ($R_2P(S)P(S)R_2$: R = ethyl, butyl), Tutunjian and Waugh[37] found that the ^{31}P–^{31}P indirect spin–spin coupling was anisotropic, with values for ΔJ between 2.2 and 3.5 kHz. They also found that J was approximately axially symmetric along the P–P bond. The ^{31}P–^{31}P J coupling in solid $Ag_4P_2O_6$ was also reported to be significantly anisotropic, where $\Delta J = +800$ Hz.[38] Anisotropies in J between ^{31}P and ^{19}F of approximately +3.0 kHz were determined for the FPO_3^{2-} group in several fluorophosphonates from ^{31}P static powder spectra.[39] A liquid crystal and X-ray diffraction study of $(CH_3)_3P{=}Se$ determined an anisotropy in the ^{31}P–^{77}Se J coupling of −680 Hz,[40] possessing the same absolute sign as $^1J_{iso}(^{31}P,^{77}Se)$.

Anisotropies in J between ^{199}Hg and other nuclei have also received some attention, such as the coupling between ^{199}Hg and ^{13}C in dimethylmercury.[18b] Although there was some variation with the solvent system used, this liquid crystal study has reported a value of 864 Hz for $\Delta J(^{13}C,^{199}Hg)$. Solid-state NMR spectra of the metal tellurides (MTe: M = Cd, Hg, Pb) have indicated substantial anisotropies in J, ranging from −180 Hz for $\Delta J(^{113}Cd,^{125}Te)$ to −4920 Hz for $\Delta J(^{199}Hg,^{125}Te)$.[41] However, Pyykkö and co-workers[42] have questioned the choice of the sign of ΔJ in these compounds, as they find a much better correlation with their calculated values if the other choice is made. As mentioned previously, one must remember that the absolute sign of R_{eff} is not available from the solid-state NMR line shape alone,

---

(33) Penner, G. H.; Wasylishen, R. E. *Can. J. Chem.* **1989**, *67*, 1909.

(34) Buergi, H. B.; Fischer, E.; Kunz, R. W.; Parvez, M.; Pregosin, P. S. *Inorg. Chem.* **1982**, *21*, 1246.

(35) Allman, T.; Lenkinski, R. E. *Inorg. Chem.* **1986**, *25*, 3202.

(36) Power, W. P.; Lumsden, M. D.; Wasylishen, R. E. *Inorg. Chem.* **1991**, *30*, 2997.

(37) (a) Tutunjian, P. N.; Waugh, J. S. *J. Chem. Phys.* **1982**, *76*, 1223. (b) Tutunjian, P. N.; Waugh, J. S. *J. Magn. Reson.* **1982**, *49*, 155.

(38) Grimmer, A.-R.; Peter, R.; Fechner, E. *Z. Chem.* **1978**, *18*, 109.

(39) (a) Grimmer, A.-R.; Müller, D.; Neels, J. *Z. Chem.* **1983**, *23*, 140. (b) Haubenreisser, U.; Sternberg, U.; Grimmer, A.-R. *Mol. Phys.* **1987**, *60*, 151.

(40) Cogne, A.; Grand, A.; Laugier, J.; Robert, J. B.; Wiesenfeld, L. *J. Am. Chem. Soc.* **1980**, *102*, 2238.

(41) (a) Nolle, A. *Z. Physik B* **1979**, *34*, 175. (b) Balz, R.; Haller, M.; Hertler, W. E.; Lutz, O.; Nolle, A.; Schafitel, R. *J. Magn. Reson.* **1980**, *40*, 9.

(42) Viste, A.; Hotokka, M.; Laaksonen, L.; Pyykkö, P. *Chem. Phys.* **1982**, *72*, 225.

although other information, such as the internuclear separation and absolute sign of J, can be used to limit the possible values for ΔJ.

In light of this work and the results available in the literature, from both experimental and theoretical investigations, it is clear that there are significant anisotropies in the indirect spin–spin coupling involving heavier elements of the periodic table. Such observations conclusively show that these couplings are not determined solely by contact terms and that interpretations based upon this assumption need to be reevaluated. It may be revealed, after further effort, that the trends in J couplings previously proposed from solution studies are indeed primarily due to variations in the contact terms. However, at present, there is no evidence to support this, due in part to the paucity of experimental data for ΔJ. We believe that the examples presented here provide unequivocal evidence for the magnitude of ΔJ in these compounds. It is hoped that investigations such as that performed here will continue and increase our knowledge of the origins and factors determining the nature of the indirect spin–spin coupling between nuclear spins.

Acknowledgment. We thank the Natural Sciences and Engineering Research Council (NSERC) of Canada for financial support in the form of operating and equipment grants (R.E.W.) and scholarship assistance (W.P.P.). The NSERC also supports the Atlantic Region Magnetic Resonance Centre, where all spectra were obtained. We also appreciate the assistance of Dr. A. Berger and Dr. A. Kentgens in providing software to aid in the fitting of slow-spinning MAS spectra and Prof. G. Penner for providing some of the preliminary experimental spectra.

Force Field Design for Metalloproteins

Stephen C. Hoops,[†] **Kenneth W. Anderson,**[‡] **and Kenneth M. Merz, Jr.***

Contribution from the Department of Chemistry and Molecular and Cell Biology, The Pennsylvania State University, University Park, Pennsylvania 16802. *Received April 1, 1991*

Abstract: Herein we describe a general approach to systematic derivation of force field parameters for metalloproteins. In particular, we have extended the AMBER force field to model the zinc ion in human carbonic anhydrase II (HCAII) in both the high (zinc–hydroxide) and low (zinc–water) pH forms. Key elements of this approach are the systematic evaluation of molecular orbital methods for modeling the metallic center (zinc in HCAII) with its ligands in the active site and the force field representation of electrostatic interactions with point charges fitted to the electrostatic potential. The resulting greater accuracy in modeling electrostatic interactions for the active site embedded in the protein environment increases the capacity for studying the static and dynamic structure of human carbonic anhydrase II. This approach should be transferable to computational studies of other metalloproteins at fixed coordination numbers.

Introduction

Several force fields have been developed in order to conduct computer simulations of the structure and function of proteins.[1-6] In general these force fields have undergone continuous improvement, and they are increasingly useful in simulating the three-dimensional structures and dynamic properties of proteins. Herein we describe the application of a systematic method for accurately incorporating a metal ion and its ligands into a classical force field for subsequent modeling of the static and dynamic structure of a metalloprotein.

The present study utilizes and builds upon the AMBER force field.[1] In this force field the total energy of the system is modeled by the potential function.

$$E_{\mathrm{Total}} = \sum_{\mathrm{bonds}} \frac{K_r}{2}(r - r_{\mathrm{eq}})^2 + \sum_{\mathrm{angles}} \frac{K_\theta}{2}(\theta - \theta_{\mathrm{eq}})^2 + \sum_{\mathrm{dihedrals}} \sum_{n} \frac{V_n}{2}[1 + \cos(n\theta - \gamma)] + \sum_{i<j} \epsilon_{ij}\left[\left(\frac{R_{ij}^*}{R_{ij}}\right)^{12} - \left(\frac{R_{ij}^*}{R_{ij}}\right)^{6}\right] + \frac{1}{\mathrm{VDW}_{\mathrm{scale}}} \sum_{\substack{i<j \\ \text{1-4 terms}}} \epsilon_{ij}\left[\left(\frac{R_{ij}^*}{R_{ij}}\right)^{12} - \left(\frac{R_{ij}^*}{R_{ij}}\right)^{6}\right] + \sum_{\text{H-bonds}}\left[\frac{C_{ij}}{R_{ij}^{12}} - \frac{D_{ij}}{R_{ij}^{10}}\right] + \sum_{i<j} \frac{q_i q_j}{\epsilon R_{ij}} + \frac{1}{EE_{\mathrm{scale}}} \sum_{\substack{i<j \\ \text{1,4 terms}}} \frac{q_i q_j}{\epsilon R_{ij}}$$

The first three terms present energy contributions for the internal motions, bond stretching, angle bending, and dihedral torsions, present in the molecule. The fourth and fifth terms (Lennard-Jones terms) represent the nonbonded interactions between atoms separated by distance R, and the sixth term represents hydrogen-bonding interactions. The last two terms shown represent the contributions to potential energy due to electrostatic interactions between point charges q_i and q_j separated by distances R_{ij} in a medium of dielectric constant ϵ. The assignment of point charges can be a critical problem in modeling proteins. In metalloproteins the presence of the metallic ion produces particularly strong electrostatic interactions which can be a major influence in determining the three-dimensional structure, modes of binding between small molecule and ion substrates, and mechanisms for catalysis.[7] The accurate modeling of these last two electrostatic terms for metalloenzymes will be an important focus of this article.

Force field calculations can be coupled with other computational techniques, such as molecular dynamics (MD),[8,9] quantum me-

---

[†] Present address: The Pennsylvania State University, New Kensington Campus, New Kensington, PA 15068.

[‡] Participant in the National Science Foundation Research Experience for Undergraduates Program.

(1) (a) Weiner, S. J.; Kollman, P. A. *J. Comput. Chem.* **1986**, *6*, 718. (b) Singh, U. C.; Ghio, C.; Alagona, G.; Profeta, S., Jr.; Weiner, P. *J. Am. Chem. Soc.* **1986**, *7*, 230.

(2) Brooks, B. R.; Bruccoleri, R. E.; Olafson, B. D.; States, D. J.; Swaminathan, S.; Karplus, M. J. *J. Comput. Chem.* **1983**, *4*, 187.

(3) Hermans, J.; Berendson, J. C.; van Gunsteren, W. F.; Potsma, J. P. M. *Biopolymers* **1984**, *23*, 1513.

(4) Momany, F.; McGuire, R.; Burgess, A.; Scheraga, J. *J. Phys. Chem.* **1975**, *79*, 2361.

(5) Jorgensen, W. L.; Tirado-Rives, J. *J. Am. Chem. Soc.* **1988**, *110*, 1657.

(6) Merz, K. M., Jr.; Kollman, P. Unpublished results.

(7) See for example: Burley, S. K.; Petsko, G. A. *Adv. Protein Chem.* **1988**, *39*, 125. Harvey, S. C. *Proteins: Struct. Func. Genet.* **1989**, *5*, 78. Davis, M.; McCammon, J. A. *Chem. Rev.* **1990**, *90*, 509 and references cited therein.

(8) Brooks, C. L., III; Karplus, M.; Pettitt, B. M. *Advances in Chemical Physics. Volume LXXI: Proteins: A Theoretical Perspective of Dynamics, Structure, and Thermodynamics*; John Wiley and Sons: New York, 1988.

(9) McCammon, J. A.; Harvey, S. C. *Dynamics of Proteins and Nucleic Acids*; Cambridge University Press: New York, 1987.

0002-7863/91/1513-8262$02.50/0